



# Synthesis, structure and luminescence properties of lanthanide complex with a new tetrapodal ligand featuring salicylamide arms

Xue-Qin Song<sup>a,b</sup>, Xiao-Guang Wen<sup>b</sup>, Wei-Sheng Liu<sup>a,\*</sup>, Da-Qi Wang<sup>c</sup>

<sup>a</sup> College of Chemistry and Chemical Engineering and State Key Laboratory of Applied Organic Chemistry, Lanzhou University, Lanzhou 730000, China

<sup>b</sup> School of Chemical and Biological Engineering, Lanzhou Jiaotong University, Lanzhou 730070, China

<sup>c</sup> Department of Chemistry, Liaocheng University, Liaocheng 252000, China

## ARTICLE INFO

### Article history:

Received 29 March 2009

Received in revised form

1 July 2009

Accepted 12 July 2009

Available online 31 August 2009

### Keywords:

Lanthanide coordination polymer

Salicylamide

Crystal structure

Hydrogen-bond

Luminescence properties

## ABSTRACT

A new tetrapodal ligand 1,1,1-tetrakis[[(2'-(2-furfurylaminoformyl))phenoxy]methyl]methane (L) has been prepared and their coordination chemistry with  $Ln^{III}$  ions has been investigated. The structure of  $\{[Ln_4L_3(NO_3)_{12}] \cdot H_2O\}_\infty$  ( $Ln = Nd, Eu$ ) shows the binodal 4,3-connected three-dimensional interpenetration coordination polymers with topology of a  $(8^6)_3(8^3)_4$  notation.  $[DyL(NO_3)_3(H_2O)_2] \cdot 0.5CH_3OH$  and  $[ErL(NO_3)_3(H_2O)(CH_3OH)] \cdot CH_3COCH_3$  is a 1:1 mononuclear complex with interesting supramolecular features. The structure of  $[NdL(H_2O)_6] \cdot 3ClO_4 \cdot 3H_2O$  is a 2:1 mononuclear complex which further self-assembled through hydrogen bond to form a three-dimensional supramolecular structures. The result presented here indicates that both subtle variation of the terminal group and counter anions can be applied in the modulation of the overall molecular structures of lanthanide complex of salicylamide derivatives due to the structure specialties of this type of ligand. The luminescence properties of the  $Eu^{III}$  complex are also studied in detail.

© 2009 Elsevier Inc. All rights reserved.

## 1. Introduction

The design and construction of polymeric metal-organic hybrid complexes are of considerable interest in recent years, due to their appealing structural topologies and potential application in catalysis, adsorption/separation, host-guest chemistry, and the promising photo-, electro-, and magnetofunctional materials [1–3]. Metal-organic frameworks containing lanthanide ions as connectors is particularly attractive because of the magnetic and electronic properties of  $4f$  ions, which should result in the application of lanthanide polymers in sensors, lighting devices, and optical storage [4]. Lanthanide ions, with their high coordination flexibility and their lack of preferential geometries, are good candidates to provide unique opportunities for the discovery of unusual network topologies [5–7], thus leading us to this interesting and challenging field. So far, much work is focused on using multicarboxylate ligands to prepare lanthanide-containing MOFs [8,9]. By contrast, based on a query to the Cambridge Structural Database (CSD), we find that the synthesis of multi-dimensional lanthanide-containing MOFs by using amide ligands is less developed [10].

Owing to the structural features of salicylamide derivatives which afforded diverse types of lanthanide supramolecular complexes upon variation of the backbone and terminal groups,

some lanthanide complexes with intriguing structure as well as interesting luminescence properties have been reported [11]. In order to further understand the influence on the structure as well as the regularity of luminescence properties of their complexes, it is necessary to extend such a studying area for improving desirable properties. At the same time, we have tried to merge the role of anions in this self-assembly. As a part of our systematic investigation of self-assembly based on salicylamide ligands, we report herein the synthesis of a new tetrapodal ligand featuring salicylamide arms, namely, 1,1,1-tetrakis[[(2'-(2-furfurylaminoformyl))phenoxy]methyl]methane (L) and describe the synthesis and crystal structure of the resulting complexes. Two three-dimensional polymeric coordination complexes, namely,  $[Nd_4L_3(NO_3)_{12} \cdot 6H_2O]_\infty$ ,  $\{[Eu_4L_3(NO_3)_{12}] \cdot 6H_2O\}_\infty$ , three mononuclear complex with interesting supramolecular properties, namely,  $\{[DyL(NO_3)_3(H_2O)_2] \cdot 0.5CH_3OH\}$ ,  $\{[ErL(NO_3)_3(H_2O)(CH_3OH)] \cdot CH_3COCH_3\}$  and  $\{[NdL_2(H_2O)_6] \cdot 3ClO_4 \cdot 3H_2O\}$ , were structurally characterized by single-crystal X-ray diffraction together with the luminescence properties of the  $Eu^{III}$  complex.

## 2. Experimental

### 2.1. Materials

The commercially available chemicals were used without further purification. All of the solvents used were of analytical reagent grade.

\* Corresponding author. Fax: +86 931 8912582.

E-mail address: [liuws@lzu.edu.cn](mailto:liuws@lzu.edu.cn) (W.-S. Liu).

## 2.2. Methods

The metal ions were determined by EDTA titration using xylenol orange as indicator. C, N and H were determined using an Elementar Vario EL. Melting points were determined on a Kofler apparatus. IR spectra were recorded on Nicolet FT-170SX instrument with pressed KBr pellets in the 400–4000  $\text{cm}^{-1}$  region.  $^1\text{H}$  NMR spectra were measured on a Bruker DRX 300 spectrometer in  $\text{CDCl}_3$  solution with TMS as internal standard. Fluorescence measurements were made on FLS920 of Edinburgh Instrument equipped with quartz cuvettes of 1 cm path length with a xenon lamp as the excitation source. An excitation and emission slit of 2.5 nm were used for the measurements of luminescence in solid state. The 77 K solution-state phosphorescence spectra were recorded with solution samples loaded in a quartz tube inside a quartz-walled optical Dewar flask filled with liquid nitrogen in the phosphorescence mode. Quantum yields were determined by an absolute method using an integrating sphere on FLS920 of Edinburgh Instrument. The luminescence decays were recorded using a pumped dye laser (Lambda Physics model FL2002) as the excitation source. The nominal pulse width and the linewidth of the dye laser output were 10 ns and 0.18  $\text{cm}^{-1}$ , respectively. The emission of a sample was collected by two lenses into a monochromator (WDG30), detected by a photomultiplier and processed by a Boxcar Average (EGG model 162) in line with a microcomputer. Reported luminescence lifetimes are averages of at least three independent determinations.

## 2.3. Crystal structure determination

X-ray single-crystal diffraction of all complexes was performed on CCD area diffractometer with  $\text{MoK}\alpha$  radiation ( $\lambda=0.71073 \text{ \AA}$ ) at 298 K. In each case, semiempirical absorption correction was applied (SADABS) and the program SAINT was used for integration of the diffraction profiles [12]. The structures were solved by direct methods using SHELXS of the SHELXL package and refined with SHELXL [13]. The non-H atoms were modeled with anisotropic displacement parameters and refined by full-matrix least-squares methods on  $F^2$ . Generally, C-bound hydrogen atoms were placed geometrically and refined as riding. Isotropic

displacement parameters of hydrogen were derived from their parent atoms. The hydrogen atoms of the water molecules were located by a difference Fourier map and refined with distance restraints for O–H and H...H (0.90 and 1.50  $\text{\AA}$ , respectively), and one variable isotropic U for  $\text{Nd}^{\text{III}}$  perchlorate complex. In the structure of  $\text{Nd}^{\text{III}}$  complex, the terminal furfurylamine group exhibits disorder over two positions and the occupancy ratios were found to 0.529/0.471. In all cases of refinements, structural restraints were applied for solvent molecules, benzene or furan rings of the ligand, the full details of which are given in the ESI CIF files. Details of crystallographic parameters, data collection and refinements are listed in Table 2. Representative bond distances and angles for  $\text{Nd}^{\text{III}}$ ,  $\text{Eu}^{\text{III}}$ ,  $\text{Dy}^{\text{III}}$ ,  $\text{Er}^{\text{III}}$  nitrate and  $\text{Nd}^{\text{III}}$  perchlorate complexes are listed in Table S1, S2 and S3, respectively. Crystallographic data for the structures reported in this paper have been deposited with the Cambridge Crystallographic Data Centre as CCDC 705664–705668.

## 2.4. Synthesis of the ligand

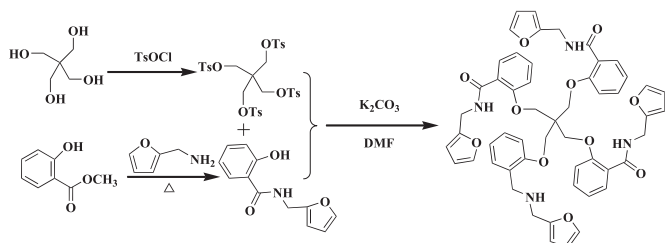
The ligand 1,1,1-tetrakis[[(2'-(2-furfurylaminoformyl))phenoxy]methyl]methane (L) (Scheme 1) was prepared similar to the literature procedure [11f]. Yield 76%. m.p.: 161.7  $^{\circ}\text{C}$ . Analytical data, Calc. for  $\text{C}_{53}\text{H}_{48}\text{N}_4\text{O}_{12}$ : C, 68.23; H, 5.19; N, 6.01; Found: C, 68.52, H, 5.21, N, 6.04; IR (KBr,  $\nu$ ,  $\text{cm}^{-1}$ ): 3417, 3314 (m, NH), 1648 (s, C=O), 1601 (m), 1537 (m), 1299 (m), 1224 (m), 750 (m).  $^1\text{H}$  NMR ( $\text{CDCl}_3$ , 300 MHz):  $\delta$ : 4.16 (s, 8H,  $\text{OCH}_2$ ), 4.48 (d,  $J=5.4$ , 8H,  $\text{NHCH}_2$ ), 6.11 (m, 8H, Ar), 6.82 (d,  $J=8.1$ , 4H, Ar), 6.98 (s, 4H, Ar), 7.13 (t, 4H, Ar), 7.20 (t, 4H, NH), 7.44 (m, 4H), 8.0 (dd, 4H, Ar).

## 2.5. Syntheses of the complexes

One millimole of ligand and 1 equiv (1 mmol) of the lanthanide nitrates or perchlorates were dissolved in a minimum methanol+acetone+ethyl acetate ( $v:v=1:1:8$ ) solution under reflux. Then the flask was cooled, and the mixture was filtered into a sealed 25–40 ml glass vial for crystallization at room temperature. After about three weeks crystals suitable for analysis were obtained. Elemental analysis data and IR spectra data characteristic of the complexes are listed in Table 1.

## 3. Results and discussion

The tetrapodal ligand was prepared by the ether base coupling of pentaerythritol benzenesulfonate and the furfurylsalicylamide in a 1:4 ratio in dry DMF in the presence of an excess of anhydrous  $\text{K}_2\text{CO}_3$  (Scheme 1). Purification of L was accomplished by column chromatography over silica, eluting with petroleum ether/ethyl acetate ( $v:v=2:1$ ) to give a pale white solid with the yield of 76%.



Scheme 1. The synthetic route of the ligand.

Table 1  
Elemental analytical and IR spectral data for the complexes.

Compound	Elemental analyses <sup>a</sup>				IR ( $\lambda_{\text{max}}/\text{cm}^{-1}$ ) $\nu$ (C=O)
	C	H	N	Ln	
$\text{Nd}_4\text{L}_3(\text{NO}_3)_{12}(\text{H}_2\text{O})_6$	45.38 (45.17)	3.70 (3.72)	7.93 (7.95)	13.59 (13.65)	1607
$\text{Eu}_4\text{L}_3(\text{NO}_3)_{12}(\text{H}_2\text{O})_6$	44.69 (44.84)	3.68 (3.69)	7.90 (7.89)	14.34 (14.27)	1606
$\text{DyL}(\text{NO}_3)_3(\text{H}_2\text{O})_2(\text{CH}_3\text{OH})_{0.5}$	48.38 (48.19)	4.10 (4.08)	7.37 (7.35)	12.12 (12.19)	1607 1644
$\text{ErL}(\text{NO}_3)_3(\text{CH}_3\text{OH})(\text{H}_2\text{O})(\text{C}_3\text{H}_6\text{O})$	49.29 (49.10)	4.37 (4.34)	7.05 (7.03)	11.96 (12.00)	1604 1632
$\text{NdL}_2(\text{H}_2\text{O})_9(\text{ClO}_4)_3$	51.41 (51.53)	4.67 (4.65)	4.52 (4.54)	5.81 (5.84)	1605 1638

<sup>a</sup> Data in parentheses are calculated values.

### 3.1. Physical measurements

The new ligand gave satisfactory  $^1\text{H}$  NMR, IR spectra and elemental analyses. Treatment of  $\text{Ln}(\text{NO}_3)_3 \cdot 6\text{H}_2\text{O}$  with the ligand in ethyl acetate–acetone–methanol solution yields a series of complexes which, according to combustion analysis (Table 1), correspond to the formula of  $\text{Ln}_4\text{L}_3(\text{NO}_3)_{12}(\text{H}_2\text{O})_6$  ( $\text{Ln}=\text{Nd}$  and  $\text{Eu}$ ),  $\text{DyL}(\text{NO}_3)_3(\text{H}_2\text{O})_2(\text{CH}_3\text{OH})_{0.5}$ ,  $\text{ErL}(\text{NO}_3)_3(\text{H}_2\text{O})(\text{CH}_3\text{OH})(\text{CH}_3\text{OCH}_3)$  and  $\text{NdL}^2(\text{H}_2\text{O})_9(\text{ClO}_4)_3$ , respectively. X-ray quality crystals of the complexes were obtained after several weeks from vapor diffusion from ethyl acetate/acetone/methanol solution. The complexes are soluble in DMF, DMSO, methanol and ethanol, slightly soluble in ethyl acetate, acetonitrile and acetone, but insoluble in  $\text{CHCl}_3$  and ether.

The characteristic band of carbonyl group of free ligand L is shown at  $1648\text{ cm}^{-1}$ . The absence of the band round  $1648\text{ cm}^{-1}$  which is instead of a new band at ca.  $1606\text{ cm}^{-1}$  in the  $\text{Nd}^{\text{III}}$  and  $\text{Eu}^{\text{III}}$  nitrate complex compared to the free ligand indicates the complete coordination of the ligand. However, the IR spectrum of  $\text{Dy}^{\text{III}}$  and  $\text{Er}^{\text{III}}$  nitrate complex as well as  $\text{Er}^{\text{III}}$  perchlorate complex confirmed the presence of both the uncoordinated and coordinated carbonyl group with a peak at ca.  $1640$  and  $1606\text{ cm}^{-1}$ . Weak absorptions observed in the range of  $2900$ – $2950\text{ cm}^{-1}$  can be attributed to the  $\nu\text{CH}_2$  of the ligand. The strong broad bands at ca.  $3402\text{ cm}^{-1}$  are ascribed to the vibration of the water ligands in the complexes.

### 3.2. Crystal structure descriptions

**Structure 1.** Prismatic crystals of  $\text{Nd}^{\text{III}}$  and  $\text{Eu}^{\text{III}}$  complex were obtained by reaction of  $\text{Ln}(\text{NO}_3)_3 \cdot 6\text{H}_2\text{O}$  and L in a 1:1 mol ratio in methanol–acetone–ethyl acetate solution. They are air stable and have a similar thermal decomposition behavior, which is reasonable since they possess the same polymeric motif. Single-crystal X-ray analyses reveal that  $\text{Nd}^{\text{III}}$  and  $\text{Eu}^{\text{III}}$  complex are isomorphous (Table 2), therefore, details will only be provided for the Nd analogue. The  $\text{Nd}^{\text{III}}$  complex of the ligand crystallizes in the cubic space group  $I-43d$ , which allows a 3-fold rotational axis passes through the  $\text{Nd}^{\text{III}}$  ion and thus to give a  $\text{C}_3$  molecular symmetry. It is also important to note that the C1 atom of the ligand lies at a

site with  $-4$  crystallographic symmetry and the water oxygen atom O7 lies on a twofold axis. Since the asymmetric building block having  $\text{C}_3$  symmetry has a tripod-type shape, and the adjacent blocks are linked by the coordination bonds of the tetrahedrally arrayed salicylamide arms of the ligand, a three-dimensional interpenetration coordination polymer formed. There is one crystallographically independent Nd atom, three fourths L ligand and three coordinated bidentate nitrate ions in each asymmetric unit as shown in Fig. 1. The three carbonyl groups from three different L ligands bridge a  $\text{Nd}^{\text{III}}$  ion, each  $\text{Nd}^{\text{III}}$  ion is thus coordinated to three carbonyl and three nitrate ions in a distorted  $[\text{NdO}_9]$  monocapped square antiprismatic coordination geometry, of which the coordination sphere for  $\text{Nd}^{\text{III}}$  is defined by three carbonyl oxygen ( $\text{Nd}-\text{O}=2.397(7)\text{ \AA}$ ) from three different

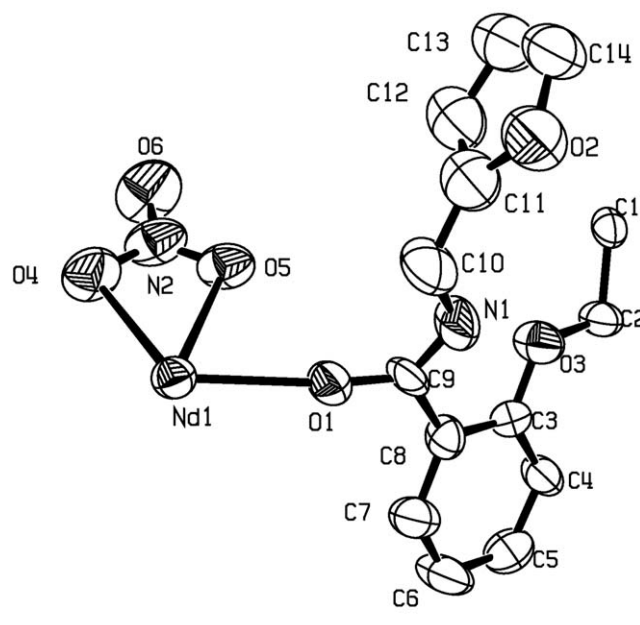


**Fig. 1.** ORTEP plot of  $\text{Nd}^{\text{III}}$  nitrate complex showing the local coordination environment of  $\text{Nd}^{\text{III}}$  with thermal ellipsoids at 30% probability (Hydrogen molecules are omitted for clarity).

**Table 2**

Crystal data and structure refinement parameters for the complexes.

Compound	1	2	3	4	5
Empirical formula	$\text{C}_{53}\text{H}_{52}\text{Nd}_1.33\text{O}_{26}$	$\text{C}_{53}\text{H}_{52}\text{Eu}_{1.33}\text{N}_8\text{O}_{26}$	$\text{C}_{53.50}\text{H}_{54}\text{DyN}_7\text{O}_{23.50}$	$\text{C}_{57}\text{H}_{60}\text{ErN}_7\text{O}_{24}$	$\text{C}_{106}\text{H}_{114}\text{Cl}_3\text{N}_8\text{NdO}_{45}$
Mr	1409.35	1419.64	1333.54	1394.38	2486.64
Crystal system	Cubic	Cubic	Monoclinic	Monoclinic	Triclinic
Space group	$I-43d$	$I-43d$	$P2(1)/n$	$P2(1)/n$	$P-1$
<i>a</i> (Å)	27.479(2)	27.520(3)	15.415(2)	16.156(4)	13.998(8)
<i>b</i> (Å)	27.479(2)	27.520(3)	21.437(3)	20.630(5)	18.871(10)
<i>c</i> (Å)	27.479(2)	27.520(3)	17.506(3)	18.210(4)	25.494(14)
$\alpha$ (°)	90	90	90	90	90.609(8)
$\beta$ (°)	90	90	95.776(2)	91.847(4)	99.710(9)
$\gamma$ (°)	90	90	90	90	102.620(8)
<i>V</i> (Å <sup>3</sup> )	20750(3)	20841(4)	5755.4(14)	6066(2)	6469(6)
<i>Z</i>	12	12	4	4	2
<i>D<sub>c</sub></i> (kg m <sup>-3</sup> )	1.353	1.357	1.539	1.527	1.277
$\mu$ (mm <sup>-1</sup> )	1.074	1.277	1.387	1.471	0.545
<i>F</i> (000)	8568	8616	2712	2844	2570
Crystal size (mm)	$0.38 \times 0.32 \times 0.21$	$0.44 \times 0.42 \times 0.39$	$0.54 \times 0.43 \times 0.40$	$0.29 \times 0.21 \times 0.18$	$0.43 \times 0.40 \times 0.27$
Data/restraints/params	3041/119/200	2929/202/189	10149/513/827	10651/288/805	22273/624/1481
Goodness-of-fit on <i>F</i> <sup>2</sup>	1.023	1.053	1.000	1.085	1.054
Final <i>R</i> indices [ <i>I</i> > 2σ( <i>I</i> )]	<i>R</i> <sub>1</sub> =0.0697 <i>wR</i> <sub>2</sub> =0.1707	<i>R</i> <sub>1</sub> =0.0860 <i>wR</i> <sub>2</sub> =0.2102	<i>R</i> <sub>1</sub> =0.0485 <i>wR</i> <sub>2</sub> =0.1374	<i>R</i> <sub>1</sub> =0.0403 <i>wR</i> <sub>2</sub> =0.0806	<i>R</i> <sub>1</sub> =0.0983 <i>wR</i> <sub>2</sub> =0.2090
<i>R</i> indices (all data)	<i>R</i> <sub>1</sub> =0.1197 <i>wR</i> <sub>2</sub> =0.2062	<i>R</i> <sub>1</sub> =0.1684 <i>wR</i> <sub>2</sub> =0.2840	<i>R</i> <sub>1</sub> =0.0825 <i>wR</i> <sub>2</sub> =0.1743	<i>R</i> <sub>1</sub> =0.0894 <i>wR</i> <sub>2</sub> =0.1094	<i>R</i> <sub>1</sub> =0.2462 <i>wR</i> <sub>2</sub> =0.2624

ligand L, six nitrate oxygen atom (Nd–O=2.519(9) and 2.543(8) Å) (Table S1, ESI). Each ligand was bonded to four nona-coordinated Nd<sup>III</sup> ions, via complexation by carbonyl oxygen donors on salicylamide arms. The Nd<sup>III</sup> ions in turn coordinated to three salicylamide arms of three other adjacent ligands, meaning that each ligand was linked by Nd coordination to four adjacent ligands. The above three-dimensional structure can also be explained by considering smaller building units. Thus, the Nd polyhedron units are connected through ligand L in three-dimensional directions, forming the three-dimensional interpenetration coordination polymers which is quite different from that reported recently [11f] showing an interesting terminal effect on structures.

Better insight into the nature of this complicated framework can also be achieved by the application of topological approach, reducing multidimensional structures to simple node and connection nets. As discussed above, in this framework, each nona-coordinated Nd<sup>3+</sup> ion is linked with three ligands through carbonyl groups, which could be considered as an inorganic trigonal node with short topological terms of 8<sup>3</sup>. Each L ligand in turn is connected with four Nd<sup>3+</sup> ions through carbonyl groups, so it could be regarded as an organic tetrahedron linker. There are six eight-membered rings around the four-connected linker, while three eight-membered rings around the three-connected metal node, resulting in a ligand linker topology of 8<sup>6</sup> as well as a metal node topology of 8<sup>3</sup>. For the four-connected linkers and three-connected nodes are arranged in a ratio of Nd/L=3:4, the short Schläfli symbol of the topology can be expressed as (8<sup>6</sup>)<sub>3</sub>(8<sup>3</sup>)<sub>4</sub> (Fig. 2) which is similar to literature [11f]. It is interesting to note that the ligand L were also arranged in exactly the same conformation as that of literature reported [11f], indicating that

the conformational freedom is apparently somewhat limited due to the steric bulk and rigidity associated with the salicylamide group.

**Structure II.** Even though the radius of Dy<sup>III</sup> is only 0.04 Å smaller than that of Eu<sup>III</sup>, the introduction of Dy<sup>III</sup> during the synthesis results a quite different product. The ligand coordinates to a single metal centre in a monodentate mode, in contrast to the tetradentate bridging coordination mode observed from the Nd<sup>III</sup> to Eu<sup>III</sup> complex possibly for the cooperative effect of the bulkier ligand, the intermolecular hydrogen bond and the smaller ionic radius which is not favorable for the ligand to replace the coordinated water molecules in this case. X-ray structural analyses revealed that the Dy<sup>III</sup> and Er<sup>III</sup> nitrate complex of ligand L formed isomorphous crystal structures (Table 2). The only minor differences are that one of the coordinated water molecule in the Dy<sup>III</sup> complex is replaced by a coordinated methanol molecule in Er<sup>III</sup> complex; the methanol solvate molecule in the Dy<sup>III</sup> complex is replaced by an acetone molecule in the Er<sup>III</sup> complex. These two complexes crystallized in the monoclinic space group *P*2<sub>1</sub>/*n* with three carbonyl O-atoms remaining uncoordinated which is quite different from that of both benzyl and pyridyl terminal group reported before [11f]. Representative bond lengths and angles are listed in Table S2 (ESI). Therefore, the structure of Er<sup>III</sup> complex was described in detail to introduce the structure II. Er<sup>III</sup> complex shows a mononuclear structure with the asymmetric unit containing one crystallographically unique Er<sup>3+</sup> ion, one neutral ligand, three bidentate nitrates, one coordinated methanol, one coordinated water molecule and one crystalline acetone molecule. A view of the molecular structure, together with its numbering scheme, is depicted in Fig. 3. The Er<sup>III</sup> atom is in a distorted [ErO<sub>9</sub>] monocapped square antiprismatic coordination geometry. Among them one oxygen atoms O2 is from carbonyl group of the ligand and the Er–O bond length is 2.244(4) Å, six oxygen atoms (O13, O14, O16, O17, O19 and O20) are from bidentate nitrate groups, and the Er–O bond lengths are 2.474(4), 2.433(45), 2.400(4), 2.427(4), 2.407(4) and 2.446(4) Å, respectively, the other two oxygen atoms O22 and O23 are from methanol and water molecular, and the Er–O bond lengths are 2.345(4) and 2.274(4) Å, respectively. All of the bond lengths for Er–O fall into normal ranges.

It is well-known that the most important driving forces in crystal engineering are coordination-bonding and hydrogen-

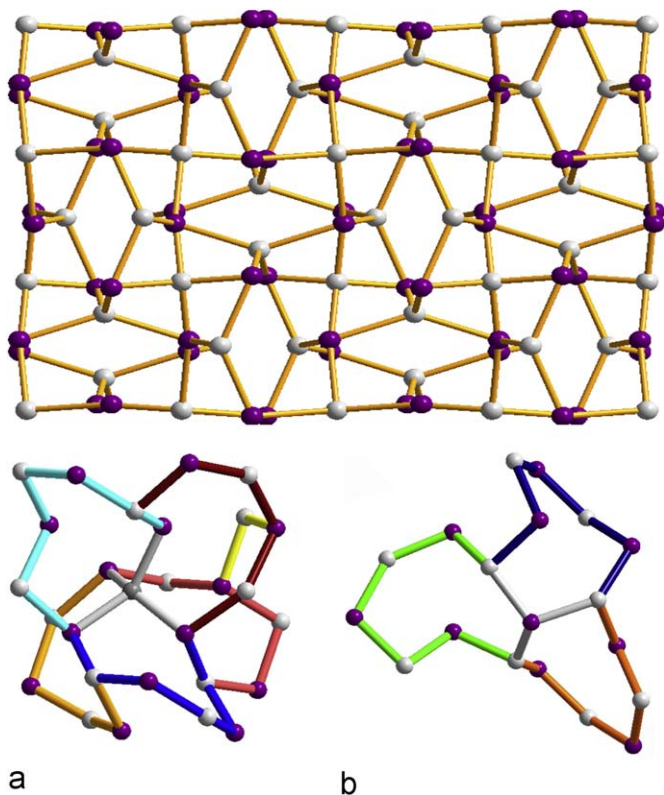


**Fig. 2.** Topological representation of the binodal (4,3)-connected (8<sup>6</sup>)<sub>3</sub>(8<sup>3</sup>)<sub>4</sub> net built on the 4-connected organic space(a) and 3-connected metal centres(b) in coordination polymer of L (the connectors of ligand L and Nd atoms are colored in gray and purple, respectively). (For interpretation of the references to colour in this figure legend, the reader is referred to the web version of this article.)

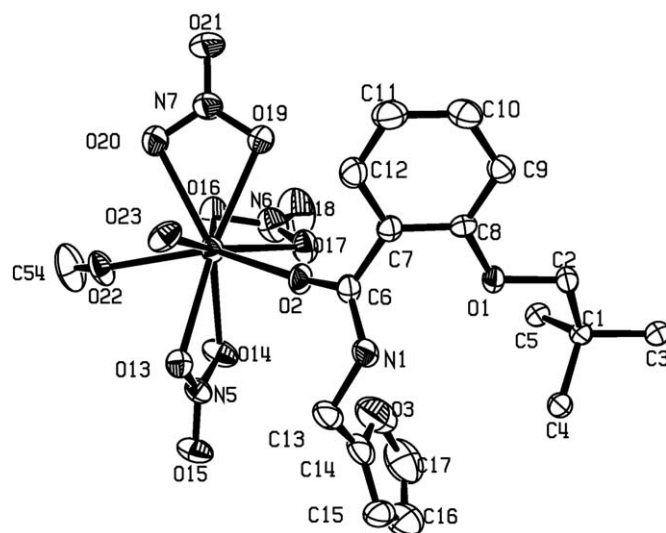


**Fig. 3.** ORTEP plot of Er<sup>III</sup> nitrate complex showing the local coordination environment of Er<sup>III</sup> with thermal ellipsoids at 30% probability (Crystalline acetone molecule and hydrogen molecules are omitted for clarity).



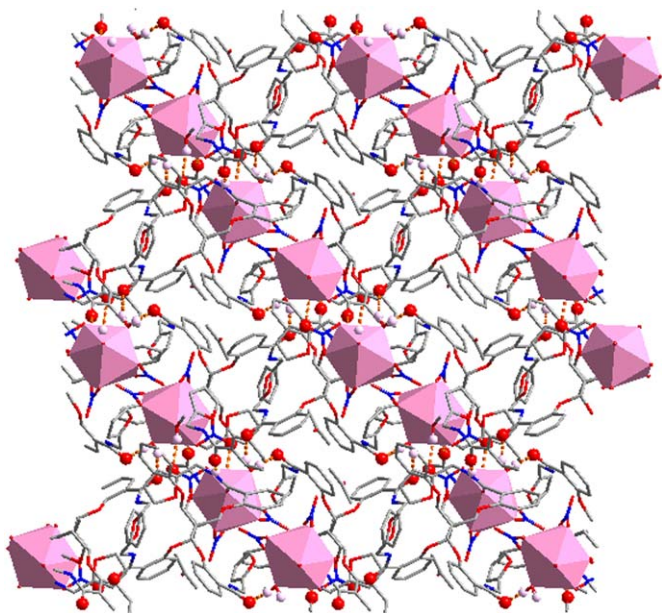


Fig. 6. The 3D supramolecular chains of  $\text{Er}^{\text{III}}$  nitrate complex constructed by hydrogen bonding which are indicated with dashed orange lines. (For interpretation of the references to colour in this figure legend, the reader is referred to the web version of this article.)

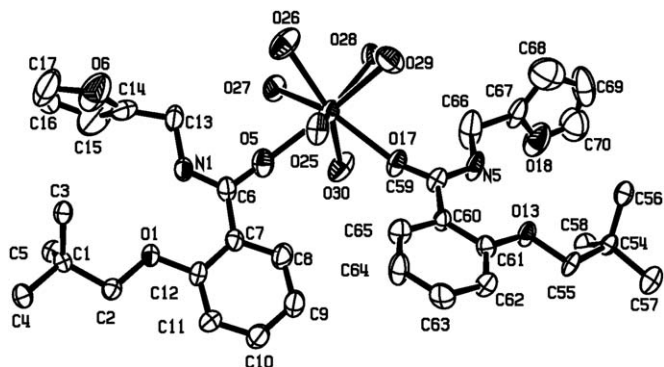


Fig. 7. ORTEP plot of  $\text{Nd}^{\text{III}}$  perchlorate complex showing the local coordination environment of  $\text{Nd}^{\text{III}}$  with thermal ellipsoids at 30% probability (Crystalline water molecule, perchlorate anion and hydrogen molecules are omitted for clarity).

three-dimensional supramolecular structures (Fig. 6). It is remarkable that the smaller ionic radii involved as well as the furan terminal group may create ligand congestion and thus effectively hinders the complete coordination of the other three carbonyl oxygen atoms of the tetrapodal ligand.

**Structure III.** To confirm the role of different counter anions in the self-assembly process of this ligand, perchlorate anions were used instead of nitrate anions to perform the reaction. In the case of the reactions of  $\text{Ln}(\text{ClO}_4)_3 \cdot 9\text{H}_2\text{O}$  with L in ethyl acetate/acetone/methanol solution, pale purple crystalline  $\text{Nd}^{\text{III}}$  perchlorate complex was obtained. A representative molecular structure plot of  $\text{Nd}^{\text{III}}$  perchlorate complex together with its numbering scheme, is depicted in Fig. 7. Compared to  $\text{Nd}^{\text{III}}$  nitrate complex, the  $\text{Nd}^{\text{III}}$  perchlorate complex crystallizes in the triclinic space group  $P\bar{1}$  and the coordination ratio of ligand to metal is 2:1. Representative bond lengths and angles are listed in Table S3 (ESI). The metal ion is 8-fold coordinated by two ligands, six water molecules with the  $\text{Nd}^{\text{III}}$  ion sitting on a crystallographic inversion centre, the perchlorate anions uncoordinatedly exist in the lattice to balance the charge. The distances Nd–O are in the range

2.357(7)–2.514(6) Å and the  $\text{Nd}^{\text{III}}$  coordination polyhedron is fairly distorted and best described as an anti-square prism. The  $[\text{NdL}(\text{H}_2\text{O})_6]^{3+}$  units self-assemble via intermolecular N3–H3...O11 and N6–H6...O21 hydrogen-bonding interactions where amide act as a N–H hydrogen-bond donor to the carbonyl O atoms to form a zigzag chain as shown in Fig. 8. These chains are further threaded via O25–H25B...O7, O27–H27B...O19, O28–H28A...O19 and O30–H30A...O23 interchain hydrogen-bonding interactions leading to a three-dimensional (3D) supermolecular structure (Fig. 9). The representative intermolecular hydrogen bonding parameters are listed in Table 4. In addition, the intramolecular N–H...O hydrogen bonds, forming among the carbonyl oxygens, amide nitrogen atoms, aqua ligands, and perchlorate anions play a vital role in determining the crystal packing and in the construction of the extended 3D supramolecular network of  $\text{Nd}^{\text{III}}$  perchlorate complex.

**Comparison of the Structures.** Investigations of the self-assembly between lanthanide nitrate salts and perchlorate salts with the tetrapodal ligand, five novel crystal products were isolated and three types of structures were obtained. In the nitrate lanthanide complexes, the coordination number (CN) of the  $\text{Ln}^{\text{III}}$  ion is nine, and the  $\text{Ln}^{\text{III}}$  ion is located in the distorted monocapped square antiprism. In the nitrate complexes the Ln–O average bond lengths decreased from 2.486 to 2.383 Å with an increase in atomic number which should be ascribed to the lanthanide contraction effect together with the structure transformation from structure I to structure II. Furthermore, the crystal system and space group for structure I were cubic and  $I\bar{4}3d$  as well as monoclinic and  $P21/n$  for structure II. Compared with the structure constructed with the related ligands [11f], the coordination behavior of L was dramatically changed due to the presence of four furan rings which affect the coordination mode of the resulting tetrapodal ligand. The formation of 3D interpenetrating network for the larger lanthanide ions takes place in a terminal group which has a weaker hydrogen-bonding acceptor, allowing the coordination of larger  $\text{Ln}^{\text{III}}$  simultaneously by the four salicylamide arms of the ligands and thus the assembly of the rare 3D nets with topology of a  $(8^6)_3(8^3)_4$  notation. The type of counter anion-dependent structural variation can be understood taking into account the plastic coordinative behaviour of the ligand, modulated by the introducing five-membered furan ring at the salicylamide arms combined with the poor coordinated and large perchlorate anion as compared to the nitrate complexes. Clearly, these unusual structural variations are an indication of cooperative effect of overall complexity of the coordination chemistry involved with this class of ligand and the lanthanide contraction as well as counter anions. The binding of lanthanide ions to the carbonyl oxygen atoms of ligands rather than to etheric oxygen groups appears largely as a consequence of cooperative effect of strong intramolecular hydrogen bonds and steric hindrance inhibiting the formation of a reasonable coordination geometry that involves the participation of all four ether oxygen donors of each ligand similar to the reported before [11]. Given the important steric demand and rigidity that the salicylamide group represents, this scenario seems rather unlikely.

### 3.3. Luminescence properties of the $\text{Eu}(\text{III})$ complex in the solid state

Upon UV irradiation, the free ligand emits a strong blue luminescence (apparent  $\lambda_{\text{max}}$  at ca. 450 nm) that can be easily detected with the naked eyes. However, upon complexation with  $\text{Eu}^{\text{III}}$  this emission is replaced by the typical luminescence color arising from  $\text{Eu}^{\text{III}}$  cation. To examine the ability of the ligand to be antenna groups for sensitized luminescence from lanthanides, we measured the luminescence properties of  $\text{Eu}^{\text{III}}$  complex with the

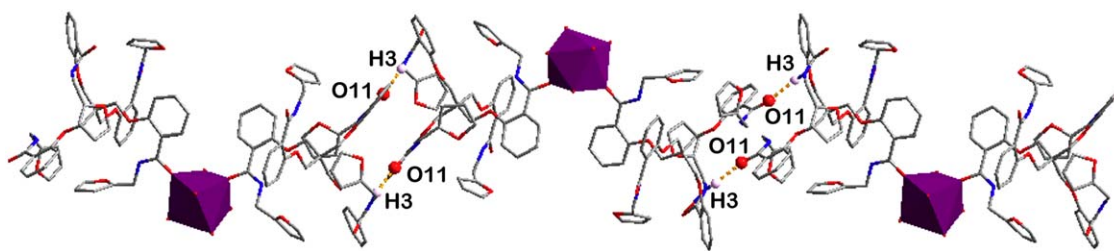


**Fig. 8.** The 1D supramolecular chains of Nd<sup>III</sup> perchlorate complex constructed by hydrogen bonding between uncoordinated carbonyl oxygen atoms and amide nitrogen atoms which are indicated with dashed orange lines. (For interpretation of the references to colour in this figure legend, the reader is referred to the web version of this article.)

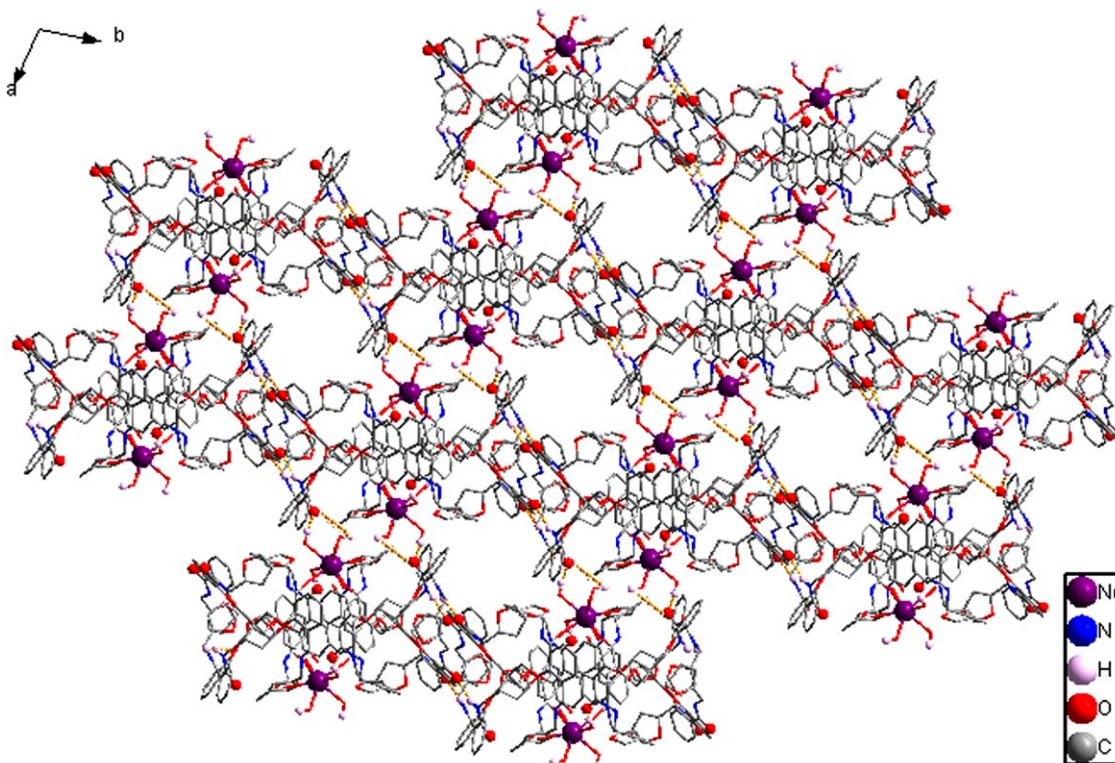


**Fig. 9.** The 3D supramolecular chains of Nd<sup>III</sup> perchlorate complex constructed by hydrogen bonding which are indicated with dashed orange lines. (For interpretation of the references to colour in this figure legend, the reader is referred to the web version of this article.)

**Table 4**

Representative intermolecular hydrogen-bonding parameters in the  $\{[\text{NdL}^2(\text{H}_2\text{O})_6] \cdot 3\text{ClO}_4 \cdot 3\text{H}_2\text{O}\}$  complex.<sup>a</sup>

D—H...A	D—H (Å)	H...A (Å)	D...A (Å)	D—H...A (°)
N3—H3...O11 <sup>i</sup>	0.86	2.08	2.848(12)	149
N6—H6...O211 <sup>ii</sup>	0.86	1.96	2.743(14)	151
O25—H25B...O7 <sup>iii</sup>	0.87	1.84	2.674(9)	161
O27—H27B...O19 <sup>iv</sup>	0.91	2.30	2.897(14)	123
O28—H28A...O19 <sup>v</sup>	0.90	1.73	2.623(12)	179
O30—H30A...O23 <sup>vi</sup>	0.88	1.84	2.675(13)	158

<sup>a</sup> Symmetry transformations used to generate equivalent atoms: (i) 1-x, -y, 1-z; (ii) 1-x, 1-y, 1-z; (iii) 1-x, 2-y, -z; (iv) -x, 1-y, -z; (v) -x, 1-y, -z; (vi) 1-x, 1-y, -z.

ligand. The excitation spectrum of the europium complex of the ligand monitoring at the emission wavelength of 579 nm exhibits a series of sharp lines characteristic of the Eu<sup>III</sup> energy-level structure, this is quite similar to the report by us before [11].

Interestingly, The luminescence emission spectra of Eu<sup>III</sup> complex only displays the metal-centred line emissions as shown in Fig. 10 which is quite different from the Eu<sup>III</sup> complex of the similar tetrapodal ligands [11f] showing a distinct terminal effect. The emission peaks of Eu<sup>III</sup> complex, at 579, 592, 619, 687 and 695 nm can be assigned to  $^5\text{D}_0 \rightarrow ^7\text{F}_j$  ( $j=0, 1, 2, 4$ ) transitions of the Eu<sup>III</sup> ion, respectively. Notably, the  $^5\text{D}_0 \rightarrow ^7\text{F}_2$  transition which is well resolved is much more intense than the  $^5\text{D}_0 \rightarrow ^7\text{F}_1$  transition, the large intensity ratio of Eu<sup>III</sup> complex for  $I(^5\text{D}_0 \rightarrow ^7\text{F}_2)/I(^5\text{D}_0 \rightarrow ^7\text{F}_1)$  indicates the absence of an inversion center at the Eu<sup>III</sup> site which is in agreement with the result of single-crystal X-ray analysis. The fluorescence quantum yield  $\Phi$  of the europium nitrate complex in solid state was found to be  $4.3 \pm 0.1\%$  using an integrating sphere. The Eu<sup>III</sup> complex luminescence decay is best described by a single-exponential process with significantly longer lifetimes of  $\tau_1 = 1.058 \pm 0.001$  ms, indicating the formation of a single species which is substantiated through X-ray single-crystal analysis (Fig. S1, ESI).

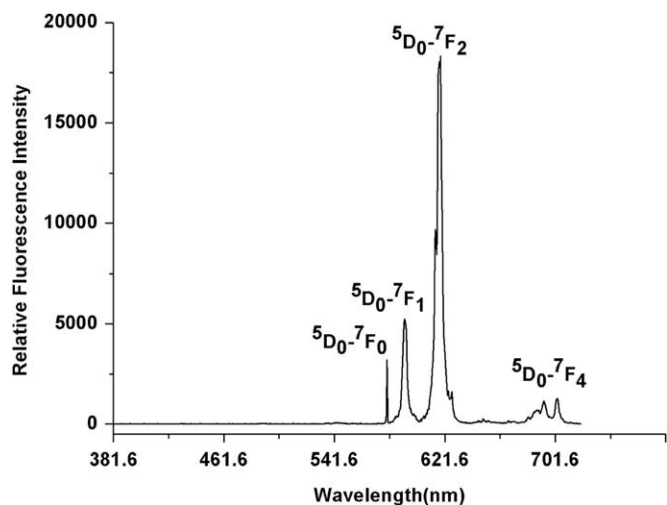


Fig. 10. Room-temperature emission spectra for  $\text{Eu}^{\text{III}}$  nitrate complex of ligand L in solid state ( $\lambda_{\text{ex}}=397$  nm, excitation and emission passes=2.5 nm).

As detailed elsewhere, the lowest  $T_{0-0}$  energy was estimated by spectral deconvolution of the 77 K luminescence signal into several overlapping Gaussian functions (Figure S2, Supporting Information) [16]. The resulting  $T_{0-0}$  energy was evaluated to be ca.  $23\,641\text{ cm}^{-1}$ . Compared with the  $\text{Eu}^{\text{III}}$  complex of the similar ligands [11f], the quantum yield and the lifetimes of  $\text{Eu}^{\text{III}}$  complex of ligand L are bigger or larger than that of ligand with pyridyl terminal group but close to that of ligand with phenyl terminal group, for the absence of OH oscillators in the lanthanide first coordination sphere, which is in perfect agreement with the proposed structural results.

#### 4. Conclusion

This study demonstrates that the new tetrapodal ligand, 1,1,1,1-tetrakis[(2'-(2-furfurylaminoformyl))phenoxy]methylmethane is capable of coordinating lanthanide ions with carbonyl oxygen atoms and generate diverse fascinating structures. The resulting polymers provide the lanthanide ions with a nona-coordination environment and prevents solvent and water molecules from entering the coordination sphere effectively resulting in an enhanced sensitization of the lanthanide due to a decrease in the vibronic quenching effect. It is worth noting that the change of terminal groups is a decisive factor in determining the coordination environments of the metal centers as well as luminescence properties which have significant influence on coordination environment. These results serve to illustrate the potential of salicylamide ligands both with regard to constructing interesting supramolecular structures and for purposes of incorporating predictable physical properties. From a more general perspective, the coupling of polymer and luminescence in a material has interesting prospects for the development of luminescence materials.

#### Supplementary material

Representative bond lengths (Å) and angles ( $^{\circ}$ ) for  $\text{Nd}^{\text{III}}$ ,  $\text{Eu}^{\text{III}}$ ,  $\text{Dy}^{\text{III}}$ ,  $\text{Er}^{\text{III}}$  nitrate and  $\text{Nd}^{\text{III}}$  perchlorate complex, the room-temperature solid state luminescence decay curves of  $\text{Eu}^{\text{III}}$  nitrate complex of ligand L and Phosphorescence spectra of  $\text{Gd}^{\text{III}}$  complex of ligand L in methanol–ethyl acetate solution at 77 K. (Tables S1,

S2 and S3, Figure S1 and Figure S2). Crystallographic data for the structural analysis have been deposited with the Cambridge Crystallographic Data Center, CCDC No. 705664–705668. Copies of this information may be obtained free of charge from the director, CCDC, 12 Union Road, Cambridge CB2 1EZ, UK (e-mail: deposit@ccdc.cam.ac.uk or www: <http://www.ccdc.cam.ac.uk>).

#### Acknowledgment

The authors acknowledge support from the National Natural Science Foundation of China Research (Grants 20771048, 20431010, 20621091 and J0630962).

#### Appendix A. Supplementary material

Supplementary data associated with this article can be found in the online version at doi:10.1016/j.jssc.2009.07.062.

#### References

- [1] (a) D. Braga, F. Grepioni, *Coord. Chem. Rev.* 183 (1999) 19; (b) S. Leninger, B. Olenyuk, P.J. Stang, *Chem. Rev.* 100 (2000) 853; (c) B. Moulton, M.J. Zaworotko, *Chem. Rev.* 101 (2001) 1629; (d) L. Carlucci, G. Ciani, D.M. Proserpio, *Coord. Chem. Rev.* 246 (2003) 247.
- [2] (a) M. Eddaoudi, D.B. Moler, H. Li, B. Chen, T. Reineke, M. O'Keeffe, O.M. Yaghi, *Acc. Chem. Res.* 34 (2001) 319; (b) O.R. Evans, W. Lin, *Acc. Chem. Res.* 35 (2002) 511; (c) M. Tominaga, S. Tashiro, M. Aoyagi, M. Fujita, *Chem. Commun.* (2002) 2038; (d) M.E. Davis, *Nature* 417 (2002) 813; (e) S.R. Batten, K.S. Murray, *Coord. Chem. Rev.* 246 (2003) 103.
- [3] (a) S.C. Zimmerman, M.S. Wendland, N.A. Rakow, I. Zharov, K.S. Suslick, *Nature* 418 (2002) 399; (b) N.L. Rosi, J. Eckert, M. Eddaoudi, D.T. Vodak, J. Kim, M. O'Keeffe, O.M. Yaghi, *Science* 300 (2003) 1127; (c) O.M. Yaghi, M. O'Keeffe, N.W. Ockwing, H.K. Chae, M. Eddaoudi, J. Kim, *Nature* 423 (2003) 705.
- [4] (a) K. Kuriki, Y. Koike, Y. Okamoto, *Chem. Rev.* 102 (2002) 2347; (b) C.L. Cahill, D.T. de Lill, M. Frisch, *Cryst. Eng. Commun.* 9 (2007) 15; (c) K.A. Gschneidner Jr., V. Pecharsky, J.-C.G. Bünzli, O. Guillou, C. Daiguebonne, *Handbook on the Physics and Chemistry of Rare Earths*, vol. 34, Elsevier, Amsterdam, The Netherlands, 2005; (d) R.J. Hill, D.L. Long, P. Hubberstey, M. Schröder, N.R. Champness, *J. Solid State Chem.* 178 (2005) 2414; (e) J.-C.G. Bünzli, C. Piguat, *Chem. Soc. Rev.* 34 (2005) 1048; (f) A.Y. Robin, K.M. Fromm, *Coord. Chem. Rev.* 250 (2006) 2127; (g) S. Faulkner, J.L. Matthews, *Comprehensive Coordination Chemistry II*, vol. 9, Elsevier, Oxford, UK, 2004, p. 913; (h) C. Piguat, J.-C.G. Bünzli, *Chem. Soc. Rev.* 28 (1999) 347; (i) R. Gheorghie, P. Cucos, M. Andruh, J.P. Costes, B. Donnadieu, S. Shova, *Chem. Eur. J.* 12 (2006) 187.
- [5] (a) W.S. Liu, T.Q. Jiao, Y.Z. Li, Q.Z. Liu, M.Y. Tan, H. Wang, L.F. Wang, *J. Am. Chem. Soc.* 126 (2004) 2280; (b) B.Q. Ma, D.S. Zhang, S. Gao, T.Z. Jin, C.H. Yan, G.X. Xu, *Angew. Chem. Int. Ed.* 39 (2000) 3644; (c) C. Serre, N. Stock, T. Bein, G. Férey, *Inorg. Chem.* 43 (2004) 3159.
- [6] (a) G. Mancino, A.J. Ferguson, A. Beeby, N.J. Long, T.S. Jones, *J. Am. Chem. Soc.* 127 (2005) 524; (b) T.M. Reineke, M. Eddaoudi, M. Fehr, D. Kelley, O.M. Yaghi, *J. Am. Chem. Soc.* 121 (1999) 1651; (c) X.D. Guo, G.S. Zhu, Q.R. Fang, M. Xue, G. Tian, J.Y. Sun, X.T. Li, S.L. Qiu, *Inorg. Chem.* 44 (2005) 3850.
- [7] (a) F. Luo, Y.X. Che, J.M. Zheng, *Cryst. Growth Des.* 6 (2006) 2432; (b) D.X. Hu, F. Luo, Y.X. Che, J.M. Zheng, *Cryst. Growth Des.* 7 (2007) 1733.
- [8] (a) T.M. Reineke, M. Eddaoudi, D. Moler, M. O'Keeffe, O.M. Yaghi, *J. Am. Chem. Soc.* 122 (2000) 4843; (b) L. Pan, K.M. Adams, H.E. Hernandez, X.T. Wang, C. Zheng, Y. Hattori, K. Kaneko, *J. Am. Chem. Soc.* 125 (2003) 3062; (c) B. Zhao, P. Cheng, X.Y. Chen, C. Cheng, W. Shi, D.Z. Liao, S.P. Yan, Z.H. Jiang, *J. Am. Chem. Soc.* 126 (2004) 3012.
- [9] (a) L. Pan, X.J. Li, Y. Wu, N. Zheng, *Angew. Chem. Int. Ed.* 39 (2000) 527; (b) T.M. Reineke, M. Eddaoudi, M. O'Keeffe, O.M. Yaghi, *Angew. Chem. Int. Ed.* 38 (1999) 2590; (c) C. Daiguebonne, N. Kerbellec, K. Bernot, Y. Gérard, A. Deluzet, O. Guillou, *Inorg. Chem.* 45 (2006) 5399; (d) C. Qin, X.-L. Wang, E.-B. Wang, Z.-M. Su, *Inorg. Chem.* 44 (2005) 7122;

- (e) Z.-H. Zhang, T. Okamura, Y. Hasegawa, H. Kawaguchi, L.-Y. Kong, W.-Y. Sun, N. Ueyama, *Inorg. Chem.* 44 (2005) 6219;
- (f) C. Marchal, Y. Filinchuk, D. Imbert, J.-C.G. Bünzli, M. Mazzanti, *Inorg. Chem.* 46 (2007) 6242;
- (g) Z. Wang, C.-M. Jin, T. Shao, Y.-Z. Li, K.-L. Zhang, H.-Q. Zhang, X.-Z. You, *Inorg. Chem. Commun.* 5 (2002) 642.
- [10] R. Sun, S.N. Wang, H. Xing, J.F. Bai, Y.Z. Li, Y. Pan, X.Z. You, *Inorg. Chem.* 46 (2007) 8451.
- [11] (a) J. Zhang, Y. Tang, N. Tang, M.-Y. Tan, W.-S. Liu, K.-B. Yu, *J. Chem. Soc. Dalton Trans.* (2002) 832;
- (b) Y. Tang, J. Zhang, W.-S. Liu, M.-Y. Tan, K.-B. Yu, *Polyhedron* 24 (2005) 1160;
- (c) X.-Q. Song, W. Dou, W.-S. Liu, Y.-L. Guo, X.-L. Tang, *Inorg. Chem. Commun.* 10 (2007) 1058;
- (d) X.-Q. Song, W.-S. Liu, W. Dou, Y.-W. Wang, J.-R. Zheng, Z.-P. Zang, *Eur. J. Inorg. Chem.* (2008) 1901;
- (e) X.-Q. Song, W.-S. Liu, W. Dou, J.-R. Zheng, X.-L. Tang, H.-R. Zhang, D.-Q. Wang, *Dalton Trans.* (2008) 3582;
- (f) X.-Q. Song, X.-Y. Zhou, W.-S. Liu, W. Dou, J.-X. Ma, X.-L. Tang, J.-R. Zheng, *Inorg. Chem.* 47 (2008) 11501.
- [12] Bruker AXS, SAINT Software Reference Manual, Madison, WI, 1998.
- [13] G.M. Sheldrick, SHELXTL NT Version 5.1. Program for Solution and Refinement of Crystal Structures, University of Göttingen Germany, 1997.
- [14] A.M. Beatty, *Coord. Chem. Rev.* 246 (2003) 131.
- [15] L. Carlucci, G. Ciani, D.M. Proserpio, A. Sironi, *J. Chem. Soc. Dalton Trans.* (1997) 1801;
- [b] Y.-B. Dong, M.D. Smith, R.C. Layland, H.-C. Loye, *J. Chem. Soc. Dalton Trans.* (2000) 775.
- [16] E.G. Moore, J. Xu, C.J. Jocher, I. Castro-Rodriguez, K.N. Raymond, *Inorg. Chem.* 47 (2008) 3105.